Efficient Numerical Model for Studying Bridge Pier Collapse in Floods

Thanut Kallaka, Ching-Jong Wang

***Abstract*—**High level and high velocity flood flows are potentially harmful to bridge piers as evidenced in many toppled piers, and among them the single-column piers were considered as the most vulnerable. The flood flow characteristic parameters including drag coefficient, scouring and vortex shedding are built into a pier-flood interaction model to investigate structural safety against flood hazards considering the effects of local scouring, hydrodynamic forces, and vortex induced resonance vibrations. By extracting the pier-flood simulation results embedded in a neural networks code, two cases of pier toppling occurred in typhoon days were re-examined: (1) a bridge overcome by flash flood near a mountain side; (2) a bridge washed off in flood across a wide channel near the estuary. The modeling procedures and simulations are capable of identifying the probable causes for the tumbled bridge piers during heavy floods, which include the excessive pier bending moments and resonance in structural vibrations.

***Keywords*—**Bridge piers, Neural networks, Scour depth, Structural safety, Vortex shedding

I. Introduction

RECENTLY, there are many reports on bridge failure by the rapid flood flows [1,2]. Some cases may be suspected of scouring effects. Sometimes debris flows along the river can increase flow density and flow pressures. Some piers and foundation structures may fail by excessive bending moments after hydrodynamic forces increase.

The hazard of scouring will depend on various geometries and sizes of hydraulic structures as it may reduce the stiffness of a bridge pier and its foundation until a failure occurs. Some of these failures may be related to the resonance between vortex frequencies and structural frequencies. The structural frequency is affected by the deep scouring too.

II. Methodology

Fig.1 and Fig.2 provide and overview of methods and procedures applied in this study, where M_D = moment demand; M_0 = moment capacity; f_{st} = Strouhal frequency; f_0 = structural frequency.

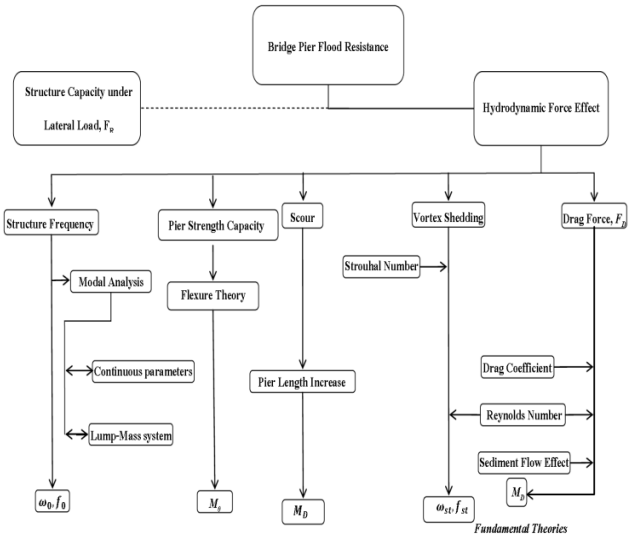

Fig. 1 Scope and methods of this study

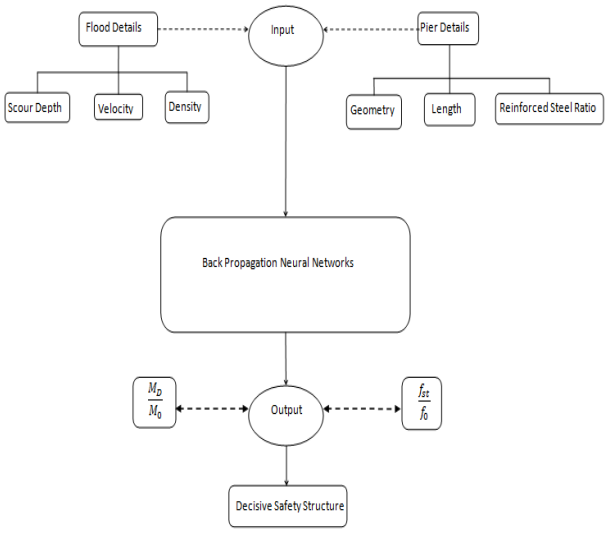

Fig. 2 Back propagation by neural networks

III. Bridge Dynamics

A long bridge structure crossing a river is a 3D MDOF system (Fig.3). The modeling and analysis for a bridge response to flow-induced forces requires a general understanding of key principles in structural dynamics. Only those related to simplified design methods applicable to regular bridge structures are reviewed in the following.

Thanut Kallaka graduated from Asian Institute of Technology, Pathumthani, 12120, Thailand (e-mail: neokmaster@hotmail.com).

Ching-Jong Wang was a visiting faculty at Asian Institute of Technology from National Kaohsiung First University of Science and Technology, Kaohsiung, 811, Taiwan (e-mail: cjw@nkfust.edu.tw).

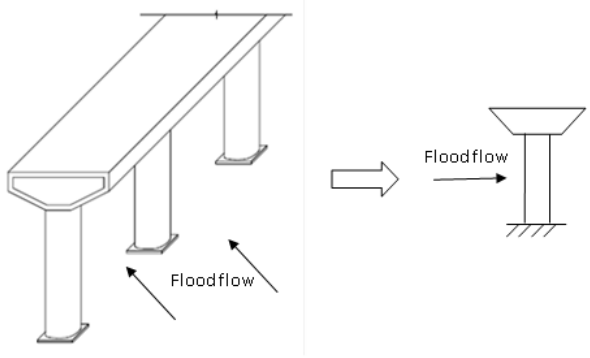

Fig. 3 Bridge dynamic model

A. Mass Calculations

Assuming a regular span of deck is simply supported on a pier bent, the pier and deck are modeled as a two-dimensional MDOF system. To capture higher mode effects, more discrete mass locations and associated DOFs are to be modeled. A simplified SDOF system is appropriate when the pier column responds to external loading mainly in a flexural mode [3]. The generalized mass of the pier and deck in the SDOF system (Fig.4) is

$$m^* = m_1 + \frac{\overline{m}_c L}{3} \tag{1}$$

where m^* = generalized mass of pier; m_1 = deck mass; $\overline{m}_c$ = distributed pier mass; L = total pier length.

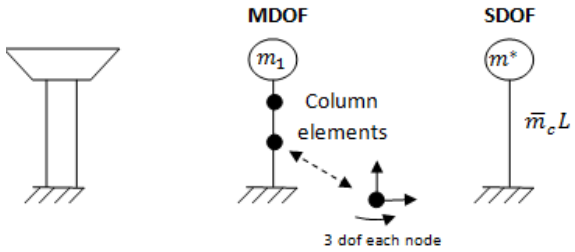

Fig. 4 Simplified pier and deck model

Given a mass m^*, a structural frequency f_0 is then determined by the pier column stiffness based on an effective moment of inertia I_e that accounts for the cracked column cross-section.

The calculation for I_e depends on axial load ratio and longitudinal reinforcement ratio. For typical circular column cross-sections, usually the typical column reinforcement ratio is between 1 and 3% and axial load ratio is between 10 and 30%. Thus, an average I_e/I_g = 50% is assumed, where I_g is the gross moment of inertia of the section [4].

C. Bending Moment Capacity

The reinforced concrete material model is from Mander et. al [4], as shown schematically in Fig.5, where strain ε and stress σ must satisfy respectively the compatibility and equilibrium conditions for a given cross-section.

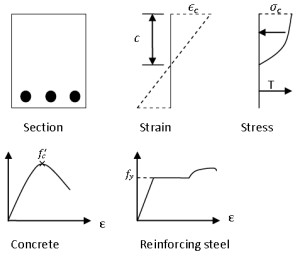

Fig. 5 Concrete and reinforcing steel behaviors

In this study, $f_c^{'} = 0.21$ Tons/cm^2 and $f_y = 4.2$ Tons/cm^2 are assumed for pier column under investigation. Some of the moment-curvature analysis results including moment capacities M_0 are shown in Fig.6 for circular sections and elliptical sections.

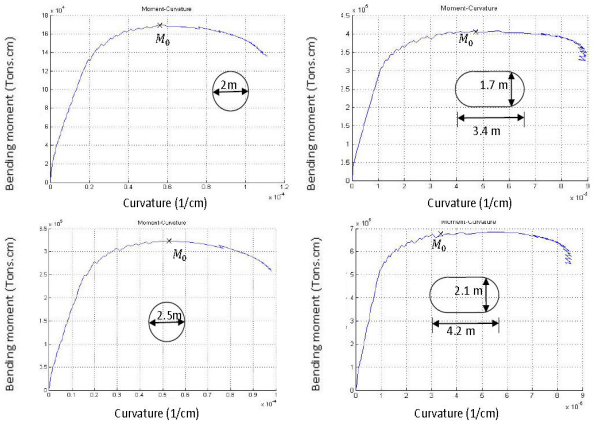

Fig. 6 Moment-curvature for pier columns (steel ratio =1.5%)

IV. Hydrodynamic Effects

A. Drag Force

The distribution of hydrodynamic pressure is as shown in Fig. 7. The hydrodynamic force is computed by the product of hydrodynamic pressure and frontal area of the immersed pier column. In this study, the water level is assumed at 90% of pier height. The average pressure P_{avg} is calculated based on empirical drag coefficient C_D [5, 6],

$$P_{avg} = \frac{1}{2} C_D \rho V_{avg}^2 \tag{2}$$

where unit of ρ = flow density in $\left[\frac{\text{Tons}}{\text{m}^3}\right]$, P_{avg} = pressure in $\left[\frac{\text{kN}}{\text{m}^2}\right]$; V_{avg} = average flow velocity in $\left[\frac{\text{m}}{\text{s}}\right]$.

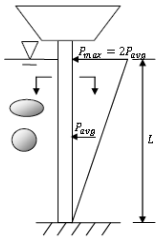

Fig. 7 Hydrodynamic drag force on piers

B. Vortex Shedding

The phenomenon of vortex shedding is characterized by the Strouhal frequency f_{st} as

$$f_{st} = \frac{St \cdot V}{D} \tag{3}$$

where St = Strouhal number; V = flow velocity; D = pier width . The Strouhal number is St a function of Reynolds number Re. This study considers St = 0.292 for $10^6 < Re < 10^7$ [7].

The velocity distribution over flow depth is as represented by a parabolic curve (Fig. 8). The vortex shedding frequency will vary as flow velocity. The occurrence of resonance between vortex shedding frequency and pier structural frequency is based on V_{avg} in an average sense [6,8].

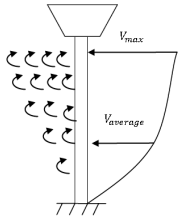

Fig. 8 Velocity distribution around pier structure

V. Efficient Simple Model

A. Scour Depth

Local scour at pier base depends on bed material gradation, flow characteristics, and geometry of pier and foundation [9,10].

The effect of scouring on pier column force will be considered in a simple model composed of deck mass, pier column, pile cap, and foundation as given in Fig. 9.

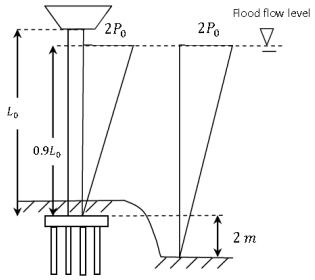

Fig. 9 A model to consider pier force due to scouring

Assume a maximum flood level at 90% of pier height and an average scour depth of 2 m below the column base.

In normal flood condition, the hydrodynamic force is

$$F_D = \frac{1}{2} \cdot 2P_{avg} \cdot A_e = P_{avg} \cdot A_e \tag{4}$$

Adding the 2-m scouring effect, it increases to

$$F_{SC} = P_{avg} A_e \left(1 + \frac{2}{0.9L_0 + 2}\right) \tag{5}$$

where L_0 is total length of the pier; A_e = frontal area for hydrodynamic force. For simplicity, the average pressure does not change by scouring.

A circular pier has 2 m in diameter and 8 m in height. The flow has a velocity of 4 m/s and density of 1.0 g/cm^3 . From drag force equation, bending moment results are as follows:

$$P_{avg} = 9.786 \times 10^{-5} \ \text{Tons} \cdot \text{cm}^{-2},$$

$$M_{SC} = 7{,}470 \ \text{Tons} \cdot \text{cm},$$

$$M_D = 6{,}764 \ \text{Tons} \cdot \text{cm}$$

where M_D = bending moment without scouring effect; M_{SC} = bending moment adding scouring effect.

These results show that the scour can cause the hydrodynamic forces to increase significantly. The shear capacity against flow force is assumed adequate for ordinary pier columns.

B. Effect on Structural Stiffness

The scour depth affects the total length of pier column and in turn affects the structural frequency. A simple model to include this effect is given in Fig.10.

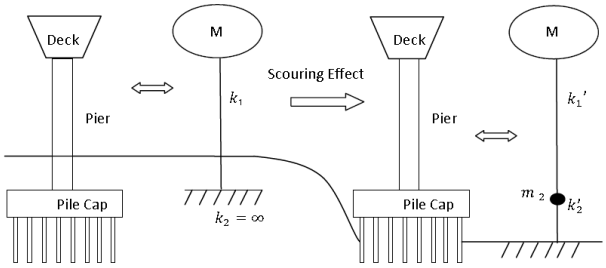

Fig. 10 A model for pier structural frequency due to scouring

The pier column stiffness changes from k_1 to $k_1^{'}$, and foundation stiffness also reduces to $k_2^{'}$. The SDOF model assumes that $m_2 = 0$ and $k_2^{'} = k_1^{'}$.

VI. Neural Network Setup

The flow parameters involve uncertainties in scour depth, flood level, flow velocity and others. Furthermore, the structural parameters also have some variations in cross-sections, pier lengths and others. To predict the probability of failure of any pier in flood, neural networks [11] are set up using more than 200 cases to train and refine. The prediction capability is only limited by the size of training data. The training algorithm is as shown in Fig.11.

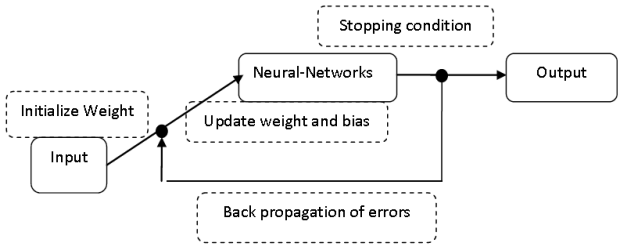

Fig. 11 Training algorithm of neural-networks

The activation function (F) for back propagation in this study is a bipolar sigmoid function as shown in Fig.12.

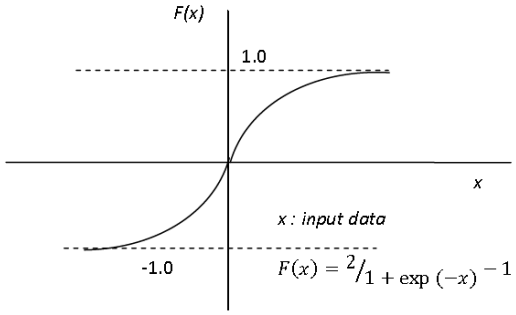

Fig.12 Bipolar sigmoid function

The results after training are presented in Fig.13 and Fig.14. The moment prediction is accurate for all ranges while the frequency ratio prediction is accurate in range of 0.7 to 1.2.

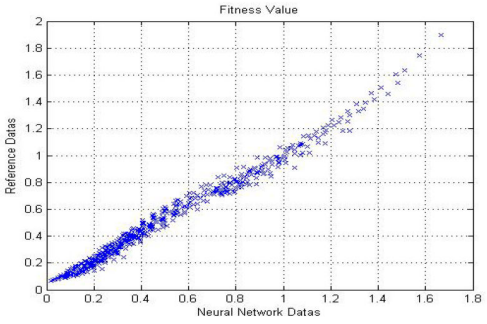

Fig. 13 Correlation for moment ratio: neural-networks vs. exact data (circular piers)

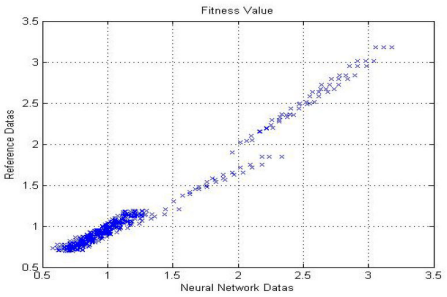

Fig. 14 Correlation for frequency ratio: neural-networks vs. exact data (elliptical piers)

VII. Cases Of Pier Failure In Flood

A. Case 1, A Bridge in Flood around Mountain areas

As shown in Fig.15, a natural reservoir is built up by incident of land slides in a mountain side. The reservoir collects rainfalls and debris until it breaks up. This situation will cause a high velocity flash flood with debris in the river downhill [2].

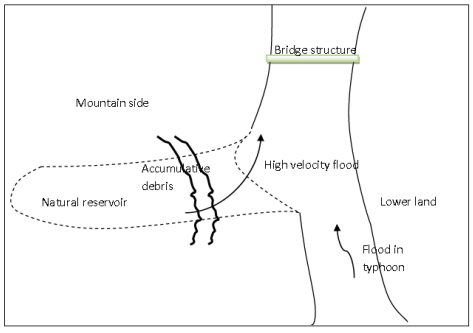

Fig. 15 Case 1: a bridge in flood around mountain areas

Debris and sludge come along during the high flood such that the flow density and flow pressure force rise much higher than normal. The increase in moment demand by deepening scour may overcome the pier's capacity. Furthermore, the vortex shedding frequency may rise to near the pier's structural frequency.

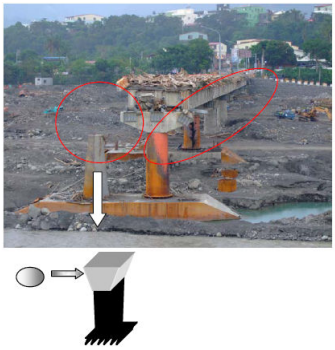

Fig. 16 Case 1: the bridge failure in flood

As shown is in Fig. 16 is a bridge with several spans washed off completely. The pier column is circular with 2 m in diameter, 10 m in height, and 1.5% of reinforcing steel. A maximum scour 2 m is assumed.

Neural networks are applied to examine all likely conditions of pier failures. The simulated results for case 1 are given in Table 1 and it shows (highlighted rows) that

1. Piers may fail by resonant vibrations from vortex shedding for a moderate flow velocity of 5 to 6 m/s.

2. Piers may fail by excessive bending moment when a flow has a high velocity (12 m/s) and large density (1.6 g/cm^3).

TABLE I
CASE 1: FAILURE CONDITIONS OF A BRIDGE IN FLOOD

Flow density (g/cm^3)	Flow velocity (m/s)	Frequency ratio (f_{st}/f_0)		Moment ratio (M_D/M_0)	
		Calculation	*Neural Networks*	*Calculation*	*Neural Networks*
1	4	0.708058	0.859531	0.068022	0.020602
1	5	0.897366	0.970805	0.106285	0.060839
1	6	1.076839	1.092205	0.15305	0.107916
1	13	2.333151	2.27053	0.718485	0.740348
1	14	2.512624	2.476797	0.833273	0.884288
1.3	4	0.717892	0.806597	0.088429	0.075942
1.3	5	0.897366	0.924392	0.13817	0.124676
1.3	6	1.076839	1.054157	0.198965	0.181772
1.3	12	2.153677	2.113239	0.795861	0.775271
1.3	13	2.333151	2.327782	0.934031	0.921956
1.3	14	2.512624	2.544806	1.083255	1.078888
1.6	4	0.717892	0.767986	0.108836	0.131415
1.6	5	0.897366	0.893434	0.170056	0.189782
1.6	6	1.076839	1.032757	0.24488	0.258179
1.6	11	1.974204	1.953862	0.82307	0.795983
1.6	12	2.153677	2.175074	0.979521	0.945161
1.6	13	2.333151	2.400678	1.149577	1.104347
1.6	14	2.512624	2.62517	1.333237	1.269203

Note that large-size drifts and floating objects may produce high impact force at the flooded deck, which is not included in this study.

B. Case 2, A Bridge in Flood near Coastal areas

As shown in Fig.17 is a stream near the estuary to the coast. Contrasted with Case 1, flood water here flows at a lesser speed and carries less debris. However, the streambed in such area usually consists of mainly fine sandy materials. As a result, a large scour depth is highly likely to cause a near-resonance from vortex induced vibration.

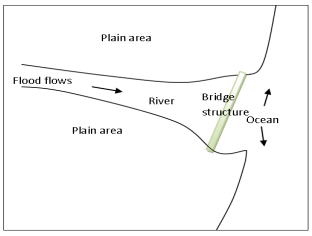

Fig. 17 Case 2: a bridge in flood around coastal areas

Fig. 18 Case 2: the bridge failure in flood

The pier column in Fig.18 has an elliptical cross-section with 1.7 m in nose diameter, 3.2 m in section depth, 8.5 m in height, and 1.5% of reinforcing steel.

TABLE II
CASE 2: FAILURE CONDITIONS OF A BRIDGE IN FLOOD

Flow density (g/cm^3)	Flow velocity (m/s)	Frequency ratio (f_{st}/f_0)	
		Calculation	*Neural Networks*
1	5	0.738353	0.812421
1	6	0.898329	0.933477
1	7	1.048051	1.063821
1	8	1.197772	1.202619
1.3	5	0.748608	0.81814
1.3	6	0.898329	0.94227
1.3	7	1.048051	1.075318
1.3	8	1.197772	1.216272
1.6	5	0.748608	0.809062
1.6	6	0.898329	0.935273
1.6	7	1.048051	1.070168
1.6	8	1.197772	1.212645

Simulated results are given in Table 2 which shows (highlighted rows) that the elliptical pier may fail due to vibrations from vortex shedding at low to moderate flow velocity of 6-7 m/s. For such elliptical piers, failure by excessive bending due to high density flow is not likely, however.

C. Case 3, An example of Thai Bridge in Flood

A flood incident caused the collapse of bridge pier columns around a hillside in Thailand. It was reported that land slides nearby had been observed.

Fig. 19 Case 3: the bridge failure in flood

The pier columns in Fig.19 have circular cross-sections with 2 m in diameter, 6 m in height, and 1.5% of reinforcing

steel. However, this structure is simplified as single pier regarding to its total stiffness and mass against flood.

TABLE III
CASE 3: FAILURE CONDITIONS OF A BRIDGE IN FLOOD

Flow density $\left(g/cm^3\right)$	Flow velocity (m/s)	Frequency ratio $\left(f_{St}/f_0\right)$	
		Calculation	*Neural Networks*
1	4	0.8403	1.0244
1	5	1.0996	1.1905
1.3	4	0.8976	0.9236
1.3	5	1.1376	1.0975
1.6	4	0.9100	0.8840
1.6	5	1.1376	1.0658

Simulated results are given in Table III which shows (highlighted rows) that the pier may fail due to vibrations from vortex shedding at low to moderate flow velocity of 4-5 m/s. For capped multi-circular piers, failure by excessive bending due to high density flow is not likely to occur.

VIII. CONCLUSIONS AND SUGGESTIONS

In this study, the failure of bridge piers in floods under effects of hydrodynamic force and scouring has been investigated. Based on a simplified model, the pier structures can be checked against failures by excessive bending moments and/or resonant vibrations.

In summary, the numerical simulations provide the most probable flow conditions that lead to the bridge failure in high floods. These conditions result from a proper combination of flow velocities, flow density, and vortex shedding, given a certain pier structural configuration. The neural networks developed can be an efficient tool for scanning similar pier structures for safety against flood induced rapid flows.

To avoid the failure by excessive bending moments or resonant vibrations in a high flood, piers of circular cross-sections are not recommended. The elliptical piers with aspect ratio of about 2.0 have shown their efficiency against high flow pressures, but the possibility of failure by vortex induced vibration during a high flood still exists.

REFERENCES

[1] Karunthanakul T., 1998. Local Scour around Row Bridge Piers. Master's Thesis. Department of Hydraulic Engineering, Chulalongkorn University.
[2] NCDR, 2010. Disaster Survey and Analysis of Morakot Typhoon (in Chinese). National Science and Technology Center for Disaster Reduction, Taiwan.
[3] Priestley M.J.N., Seible F., Calvi G.M., 1996. Seismic Design and Retrofit of Bridges. New York: John Wiley & Sons Inc.
[4] Mander J.B., Priestley M.J.N., and Park R., 1988. Theoretical Stress-Strain Model for Confined Concrete, J Struc Eng, ASCE; 114(8): 1804-26.
[5] AASHTO, 1996. Standard Specification for Highway Bridges, Sixteenth edition. American Association of State Highway and Transportation Officials.
[6] Cengel Y.A., Cimbala J.M., Fluid Mechanics, First edition, McGraw-Hill International Book Company.
[7] Roshko A. Experiments on the Flow Past a Circular Cylinder at Very High Reynolds Number. J Fluid Mech 1961; 10: 345-56.
[8] Chiu C.L., 1989. Velocity Distribution in Open Channel Flow, J Hydraulic Eng, ASCE; 115(5): 576-594.
[9] FHWA, 2001. Evaluating Scour at Bridges, Hydraulic Engineering Circular No.18. Federal Highway Administration, U.S. Department of Transportation.
[10] Sumer B.M., Fredsoe J., Christiansen N., 1992. Scour around a Vertical Pile in Wave. J waterway, Port, Coastal and Ocean Eng, ASCE; 118(1): 15-31.
[11] Flood I., Kartam N., 1994. Neural Networks in Civil Engineering: Systems and Application. J Comp in Civ. Eng, ASCE; 8(2): 131-148.

國立高雄第一科技大學
營建工程系

碩士論文

敲擊加速度反應法
應用於結構試驗

研究生：劉宇峻

指導教授：王慶忠 博士

中華民國一百年七月

敲擊加速度反應法應用於結構試驗

Structural Property Testing by Impact-Acceleration Responses

研究生　：劉宇峻　Yu-Chun Liu

指導教授：王慶忠　Ching-Jong Wang

國立高雄第一科技大學

營建工程系

碩士論文

A Thesis Submitted to
Department of Construction Engineering
National Kaohsiung First University of Science and Technology
in Partial Fulfillment of the Requirements
for the Degree of Master
in
Construction Engineering
June 2011
Yenchao, Kaohsiung, Taiwan, Republic of China

中華民國一百年七月

國立高雄第一科技大學 99 年度特色發展計畫期末報告

計畫名稱	認證及建教合作實驗室	
執行單位	營建系	
執行期間		
計畫主持人	王慶忠 老師(借調出國)、 盧之偉 老師	
經費總額	經費動支率	經費執行率
1,500,000	100%	100%

壹、背景及現況

承樊院長於經費上全額大力支持， 並考量節約公帑， 未獲支用營建系任何經費， 亦未申請本校經費聘用輔導機構， 目前本實驗室教師與研究生目前已合力完成新儀器之採購工作，因為王慶忠 老師教育部借調出國，因此本工程服務實驗室暫時由盧之偉 老師幫忙處理事情，所以若有重大事情需等王慶忠 老師回國才可處理。

貳、計畫目標

加入工學院「工程檢驗中心」，提升本校之專業公信力、建立與產業界之互動、支援教學工作，並擴大本校自籌財源之能量。

目標一以現有認證合格之混凝土鑽心試驗與低強度回填材料 CLSM 材料及施工之檢驗，加強現有設備及技術改良。目標二土壤工地密度試驗、土壤夯實試驗為一具潛力之認證項目，可配合目前國內河川防洪、整治工程積極進行。

參、具體內容及配套措施(請參考原計畫內容填寫)

1. 實驗室認證由師生合作負責，目前已能承接檢測作業，經費用於培育學生之各類實驗室專長訓練。
2. 檢測設備將可提供教師研究之用，有助提升研究能力。
3. 檢測設備將可提供營運系研究生及大學生專題，使用強化操作能力，提升學習效果。
4. 發展具營建產業特色之專業檢驗項目

肆、實施進度及分工(請參考原計畫內容填寫)

1. 進行檢測市場調查完試驗，未來之經濟效益及加強學生之就業能力與專業能力之目標。 （已完成）
2. 依據項目進行儀器增購。(本計畫)
3. 申請 TAF 之新增認證項目。(本計畫)

本實驗室將採二年分項進行認證作業，初期第一年計畫目標，將建立實驗室符合 ISO/IEC 17025 規範要求之技術文件與混凝土鑽心試驗之改良、低強度回填材料圓柱試驗之改良、混凝土圓柱模製試驗、土壤工地密度試驗、土壤夯實試驗等實驗項目合格。

伍、經費執行成果

設備名稱(中/英文)	單價	數量	金額	說明
混凝土快速研磨機 (Rapid Concrete grinding machine)	158,000	1 組	158,000	
混凝土抗壓/抗彎試驗軟體 (Concrete compressive / bending test software)	39,000	1 套	39,000	
鑽心鑽頭組(Discrepancies in the actual drill bit set)	39,000	1 組	39,000	
25 噸 CLSM 電腦伺服控制抗壓試驗機 (CLSM computer servo control 25 tons compression testing machine)	630,000	1 組	630,000	
電動液性限度儀(Electric liquid limit device)	40, 000	1 台	40, 000	
塑性限度儀(Plastic Limit device)	4, 200	1 台	4, 200	
工地密度試驗儀(Site Density tester)	14, 000	1 套	14, 000	
數位式土壤直接剪力儀(Digital soil direct shear)	430, 000	1 台	430, 000	
防水型加速度變換器(Waterproof acceleration converter)	35, 000	2 顆	70, 000	
變位變換器 (Variable bit converter)	27, 000	1 隻	27, 000	
電動液性限度儀 (Electric liquid limit device)	40, 000	1 台	40, 000	
塑性限度儀 (Plastic Limit device)	4, 200	1 台	4, 200	

陸、計畫成效

預期成果達成率及目標差異度(請參考原計畫內容並配合實際情形填寫)

預期成果	實際成果	達成率 (%)	自我檢視(與原訂目標的差異，若未達成請說明原因)
整理及尋找儀器資料	公開招標	100%	
公開招標	新儀器進來	100%	
新儀器操作步驟	廠商新儀器教育訓練	100%	
內部人員訓練	新進人員教育訓練	100%	
新儀器操作程序書	撰寫操作程序書	100%	
準備新認證	證整理資料及收集資料	30%	資料整理中

柒、實體成果照片(至少 4 張)

圖 1、25 噸 CLSM 電腦伺服控制抗壓試驗機

圖 2、混凝土快速研磨機

圖 3、數位式土壤直接剪力儀

圖 4、鑽心鑽頭組

圖 5、工地密度試驗儀

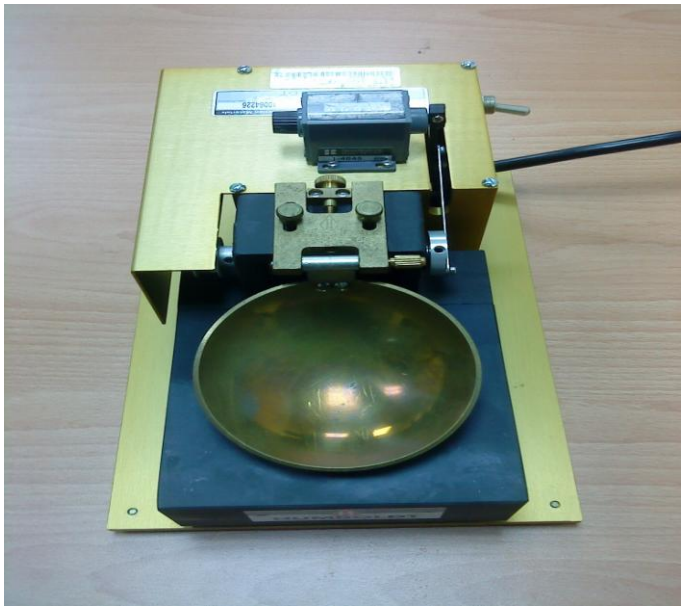

圖 5、電動液性限度儀

圖 6、塑性限度儀

圖 7-1、數位式土壤直接剪力儀操作過程

圖 7-2、數位式土壤直接剪力儀操作過程

圖 8-1、混凝土快速研磨機試驗過程

圖 8-2、混凝土快速研磨機試驗過程

圖 8-3、混凝土快速研磨機試驗過程

計畫主持人簽章：

單位主管簽章(院及系所)：